Available online at www.sciencedirect.com
ScienceDirect
Remote Sensing of Environment 112 (2008) 998–1009
Remote Sensing of Environment
www.elsevier.com/locate/rse

Mapping incident photosynthetically active radiation from MODIS data over China

Ronggao Liu [a,*], Shunlin Liang [b], Honglin He [a], Jiyuan Liu [a], Tao Zheng [b]

[a] The State Key Laboratory of Resources and Environmental Information System, Institute of Geographical Sciences and Natural Resources Research, Chinese Academy of Sciences, Beijing, China
[b] Department of Geography, University of Maryland, College Park, MD, USA

Received 10 July 2006; received in revised form 3 July 2007; accepted 15 July 2007

Abstract

Photosynthetically active radiation (PAR) is a key input parameter for almost all terrestrial ecosystem models, but the spatial resolution of current PAR products is too coarse to satisfy regional application requirements. In this paper, we present an operational system for PAR retrieval from MODIS data that is based on an idea proposed by [Liang, S., Zheng, T., Liu, R., Fang, H., Tsay, S. -C., & Running, S. (2006). Estimation of incident photosynthetically active radiation from Moderate Resolution Imaging Spectrometer data. *Journal of Geophysical Research*, 111, D15208. doi:10.1029/2005JD006730]. However, the operational system for PAR retrieval described here contains several improvements. The algorithm utilizes MODIS 1B data combining MODIS land surface products and BRDF model parameters products to directly estimate diffuse PAR, direct PAR and total PAR. Times-series data interpolation removes the noise and cloud contamination of land surface reflectance. PAR is retrieved by searching look-up tables calculated using a radiative transfer model. The system can automatically process MODIS 1B data to generate instantaneous and daily PAR. The instantaneous PAR products are compared with observational data from seven ChinaFLUX stations, and daily total PAR estimates are compared with those estimates of global radiation from 98 meteorological stations over China. The results indicate that this approach can produce reasonable PAR estimates, although this method overestimates PAR for low values of PAR.

Keywords: Photosynthetically active radiation; MODIS; China

1. Introduction

Global environmental change is one of the main problems facing humans today. Scientists have long recognized that human activities are changing the Earth's terrestrial and atmospheric systems. Conversely, these changes also affect human living conditions. To understand the interaction between the human and natural environment, various models, such as terrestrial biogeochemistry (Running et al., 1999), global vegetation biogeography (Prince & Goward, 1995), and land–atmosphere exchange process (Sellers et al., 1996) models, were used to simulate the cycles of carbon, water, nitrogen and energy in different natural systems. Since photosynthesis is the core process for energy exchange between the atmosphere and the terrestrial system, the photosynthetically active radiation (PAR), as the key part of photosynthesis process controlling the vegetation production, usually is required as an input for modeling photosynthesis from single plant leaves to complex plant communities. For example, Monteith (1972) suggested that net primary production under non-stressed conditions is linearly related to the amount of PAR that is absorbed by the green foliage.

China, one of the most populous countries and most ancient civilizations in history, is the most rapidly developing economy in the last 20 years. In response to the Kyoto Protocol appeal, the Chinese government has taken many steps to increase carbon sequestration in the terrestrial ecosystem to mitigate the global warming. Chinese forests are thought to be some of the most important forest sinks on Earth, although estimates of the amount of carbon sequestered in all of China's terrestrial carbon sinks vary considerably, from a net sink of 0.02 PgC year^{-1}

* Corresponding author. Tel.: +86 10 64889466; fax: +86 10 64855049.
E-mail addresses: lronggao@yahoo.com, liurg@lreis.ac.cn (Ronggao Liu).

0034-4257/$ - see front matter © 2007 Elsevier Inc. All rights reserved.
doi:10.1016/j.rse.2007.07.021

(Fang et al., 2001) to 0.1 PgC year^{-1} (Streets et al., 2001). Nevertheless, these estimates depend mainly on forests distribution. Few scientists have considered the effect of radiation on carbon sequestration in forests, although similar research has been conducted in other fields. Chameides et al. (1999) concluded that the air pollution in China, which reduces ground radiation, would have a large negative impact on Chinese agricultural production. Graham et al. (2003) suggested that the increase in aerosols from human activities and tropical clouds, which decrease PAR, would inhibit the photosynthesis of vegetation. However, Stanhill and Cohen (2001) argued that there was no evidence that any alteration in radiation affects agriculture, even though solar radiation on Earth has decreased about 20% in the past 50 years. Moreover, Gu et al. (2003) demonstrated that, though aerosols can reduce the direct solar radiation at the Earth's surface, they can also increase the amount of diffuse solar radiation, which play a more significant role in vegetation photosynthesis, especially for dense vegetation. Cohan et al. (2002) argued that if the diffuse radiation increase from aerosols was considered, the impact of pollution on Chinese agriculture is not as serious as Chameides et al. (1999) estimated. The radiation data that Chameides et al. (1999) and Cohan et al. (2002) used were derived from model simulations of only a small number of ground observations and model simulation, which are inexact and subject to large uncertainties. More accurate PAR data would provide a better understanding of the carbon sink/pool and its variable response to climate variability in China.

Usually, PAR is estimated from global radiation observed by meteorological stations then interpolated to cover a large area. However, only a few routinely operational meteorological stations observe global radiation, which density is too low for accurate spatial interpolation. Sometimes, the global radiation for those unavailable stations can also be estimated by models from other observed parameters, such as temperature, precipitation and air temperature (Winslow et al., 2001). This indirect method of estimation almost certainly contains large errors. Therefore, estimation of PAR from remote sensing data has become the preferential choice. Frouin and Pinker (1995) reviewed the methods for estimating incident PAR from ISCCP (International Satellite Cloud Climatology Project) and TOMS (Total Ozone Mapping Spectrometer) observations. Dye and Shibasaki (1995) compared the PAR products from ISCCP-BR, ISCCP-PL and TOMS PAR with ground data and found the RMS differences of 28.1%, 13.7%, and 7.2% respectively. High-resolution PAR data over land surfaces are still currently unavailable. The MODIS team has to disaggregate the NASA Data Assimilation Office (DAO) assimilated PAR product of 3-hourly 2° by 2.5° spatial resolution to drive the BIOME-BGC model to generate 1 km Net Primary Productivity (NPP) and net photosynthesis (PSN) products (Running et al., 1999; Zhao et al., 2005). PAR data with so low spatial resolution are not enough for regional applications.

The amount of solar radiation that reaches the Earth's surface is mainly determined by atmospheric conditions. If atmospheric components, such as ozone, vapor, aerosols, and clouds, have been determined, PAR can be estimated simply by a radiative transfer model. However, satellite observations are a mix of atmosphere and Earth surface signals, from which the atmospheric parameters and the land surface reflectances must be decoupled. Several atmospheric products have been developed by the MODIS scientist team and can be downloaded freely from NASA DAAC (http://daac.gsfc.nasa.gov), which can be used to estimate PAR over land by a simple algorithm (Van Laake & Sanchez-Azofeifa, 2004). However, these MODIS products, which are retrieved mainly from single scene data, contain many uncertainties. For example, the MODIS aerosol products are unavailable over bright land surfaces or for heavy aerosols (Remer et al., 2005). In such circumstance, PAR derived from atmospheric products is overestimated. To retrieve aerosols over variable surfaces, multi-temporal data methods, that use the minimum visible band data to represent the land surface reflectances with no atmospheric contamination, have been developed (Borde & Verdebout, 2003; Hsu et al., 2004; Hauser et al., 2005). The results are better than those from single scene data. Similar to these algorithms, Gu and Smith (1997) estimated PAR from GOES data and Liang et al. (2006) estimated PAR directly from the multi-temporal MODIS top-of-atmosphere (TOA) radiances, which can reduce uncertainties from atmospheric model selection. Liang et al.'s method has been validated by ground data from sites in the USA that show that the results are reasonably accurate. However, several shortcomings exist in the current multi-temporal composite based method. First, the composite period length is difficult to determine. If it is too long, the land surface would change substantially. But if it is too short, cloud effects may be serious. Second, shadows may contaminate the composite results. And, seasonal haze may always occur in some regions (Xiao et al., 2003), making it impossible to find a clear-sky pixel in the composite period.

In this paper, we describe an operational algorithm to produce PAR from MODIS satellite observational radiance (MOD02/MYD02) over China. Based on the method proposed by Liang et al. (2006), the new method estimates directly instantaneous PAR from satellite observational radiances so that the atmospheric model errors can be minimized. The land surface reflectances are from MODIS 8-day composite land surface (MOD09/MYD09) and 16-day BRDF (MOD43B1/MCD43B1) products. This is different from Liang et al.'s method that used the time-series interpolation of annual least blue band data. This new method initially generates the normalized land surface reflectance from BRDF-corrected MODIS MOD09/MYD09 by MOD43/MCD43 products. Cloud and noise pixels are removed by time-series interpolation at this stage. Then, normalized land surface reflectances are converted to the land surface reflectances having the same geometric angle as the MODIS MOD02/MYD02 data. Finally, these data are used to retrieve the instantaneous and daily PAR. There are several improvements in this method: (1) the dark-object based atmospheric correction is performed before compositing so much of the aerosol effect is removed from the MOD09/MYD09 data; (2) the cloud and shadow pixels are flagged before compositing; (3) the 8-days composite is long enough to capture many land surface changes; (4) the BRDF

effect can be corrected by MOD43/ MCD43 products; and (5) the cloud and noise pixels in the composite data are removed by time-series interpolation. This method has been integrated to MODISoft®, a software platform specialized for MODIS data processing, to generate instantaneous PAR and daily total PAR from MODIS 1B level data (Liu et al., 2007). The instantaneous and daily PAR data were compared with observational data from ChinaFLUX and meteorological stations.

The data descriptions are introduced in Section 2, algorithm in Section 3, and the products and the validation in Section 4. The summary and conclusion are provided in Section 5.

2. Dataset description

2.1. MODIS level 1B data

The MODIS twin sensors were launched on December 18, 1999 aboard the Terra satellite and on May 04, 2002 aboard the Aqua satellite respectively. Terra and Aqua are polar-orbiting satellites that cross the equator during the daytime at approximately 10:30 am and 1:30 pm local times. Both MODIS sensors were designed to have the same spectral characteristics with 36 spectral bands spanning 405–14385 nm wavelengths. Their spatial resolutions at nadir vary with band: 250 m (bands 1–2: VIS), 500 m (bands 3–7: VIS–MIR), and 1 km (bands 8–36: VIS–TIR). The geometric characters of the sensors ensure high accuracy in multi-spectral registration, multi-temporal registration, and absolute geolocation. Previous work has demonstrated that co-registration with MODIS data bias is less than 50 m (Wolfe et al., 2002).

2.2. MODIS land surface reflectance product

The MODIS land surface reflectance (MOD09/MYD09) product estimates the surface spectral reflectance for each band from satellite observational radiance as if it was measured at ground level without any atmospheric contamination (Vermote et al., 2002). The atmospheric correction is applied to all non-cloudy pixels of MODIS Level 1B bands 1–7 data with removal of the effect of atmospheric gases, aerosols, and thin cirrus clouds. The cirrus cloud effect is detected and removed by band 26. Water vapor, aerosol and ozone are corrected by MODIS atmospheric products. If aerosol data are not available in some regions, accessory climatological data is used or the correction is disregarded. Using the minimum blue minimum method, the eight days of land surface reflectances are composited to remove cloud and aerosol contamination. The quality status flags, acquired date and geometrical condition of every pixel are included in each product.

2.3. MODIS BRDF products

The spectral BRDF model provided by BRDF product (MOD43B1) is used to calculate the directional reflectance for any view or solar angle for MODIS bands 1–7. The BRDF model parameters are estimated by inverting multi-date, multi-angular, cloud-free, atmospherically corrected, surface reflectance observations acquired by MODIS in a 16-day period with a spatial resolution of 1 km. The operational MODIS BRDF algorithm makes use of a kernel-driven, linear BRDF model that relies on the weighted sum of an isotropic parameter and two functions (or kernels) of viewing and illumination geometry to determine reflectance, ρ (Schaaf et al., 2002).

$$\rho_\lambda(\theta_0,\theta,\varphi) = a_0 + a_{1f1}(\theta_0,\theta,\varphi) + a_2 f_2(\theta_0,\theta,\varphi) \tag{1}$$

where f_1 is the RossThick kernel that represents volumetric scattering from a dense leaf canopy based on a single scattering approximation of radiative transfer theory and f_2 is the LiSparse kernel which is derived from the geometric-optical mutual shadowing model and assumes a sparse ensemble of surface objects. Parameters a_0, a_1 and a_2 are coefficients of the kernels and are related to the isotropic, volumetric and geometric components respectively.

2.4. Land surface reflectance and albedo data preprocessing

Although the atmospheric correction and 8-day composite procedures were introduced in the MODIS MOD09/MYD09 data, the cloud, aerosol and other noise effects still exist. These noise pixels should be filled as an approximate value before they are used as background reflectances for PAR retrieval. The noise pixels can be removed by multi-temporal data interpolation (Lu et al., 2007). However, the land surface reflectance at the same position varies with different view, solar and azimuth angles due to the BRDF effect that makes the interpolation impossible. Therefore, all MOD09/MYD09 products should be converted to the same geometrical direction before interpolation. And all interpolated land surface reflectances should also be converted to be consistent with the geometric conditions of MOD02/MYD02 data for PAR retrieval. The MODIS MOD09/MYD09 and MOD43B1 products are combined to achieve these goals in two steps.

First, all pixels marked as bad quality or contaminated by clouds in MOD43B1 products are excluded. Pixels that contain some portion of snow cover are selected for separate processing. The good quality pixels are used to estimate the BRDF model parameters of noise pixels by the wavelet-based time series interpolation method (Lu et al., 2007). Because BRDF model parameters typically change little over short-time periods, we assume that BRDF parameters at same position are constant during a single compositing period.

Second, all MODIS MOD09/MYD09 data are normalized to the geometry of 45 degree solar zenith, zero degree view zenith and zero relative azimuth using the BRDF parameters from the 1 km no-noise MOD43B1 product. The normalized reflectance is computed as:

$$\rho_\lambda(\theta_s,\theta_v,\varphi) = \left[1 + \frac{a_1}{a_0} f_1(\theta_s,\theta_v,\varphi) + \frac{a_2}{a_0} f_2(\theta_s,\theta_v,\varphi)\right] \times \frac{\rho_\lambda(\theta_{s0},\theta_{v0},\varphi_0)}{\left[1 + \frac{a_1}{a_0} f_1(\theta_{s0},\theta_{v0},\varphi_0) + \frac{a_2}{a_0} f_2(\theta_{s0},\theta_{v0},\varphi_0)\right]} \tag{2}$$

where θ_{s0}, θ_{v0}, φ_0 are the solar zenith, the view zenith and the relative azimuth in MOD09/MYD09 product and θ_s, θ_v, φ are the normalized angles. Others variables are the same as in Eq. (1).

After normalization, all MOD09/MYD09 data have the same geometric orientations. MOD09/MYD09 data contain the data acquisition date of each pixel. With this information, all the good quality pixels are used to interpolate to acquire each day's normalized clear-sky land surface reflectance by the wavelet-based time-series interpolation method (Lu et al., 2007) as we described for MOD43B1. After these procedures, the 500 m no-noise land surface reflectances were calculated (Fig. 1). Fig. 1 shows that the described method effectively removes all cloud residual effects from reflectances. The geometric conditions of MODIS 1B data and the clear-sky background reflectances are used as input in Eq. (2) to compute background land surface reflectances for the MODIS 1B data.

3. PAR retrieval from MODIS data

3.1. Estimation of instantaneous PAR from MODIS data

The instantaneous radiation at the top of atmosphere (TOA) from the Sun, L_λ^{TOA}, can be estimated from:

$$L_\lambda^{\mathrm{TOA}} = E_{0,\lambda} \cdot \cos(\theta_s) \cdot d^2 \tag{3}$$

where d is the Earth–Sun distance; $E_{0,\lambda}$ is the exo-atmospheric radiation at wavelength λ at the standard solar–Earth distance, λ value being 400–700 nm and $E_{0,\mathrm{PAR}}$ 544 W m^2 for PAR, and θ_s is the solar zenith angle. θ_s is calculated from:

$$\cos(\theta_s) = \sin(\varphi)\sin(\delta) + \cos(\varphi)\cos(\delta)\cos(h) \tag{4}$$

where $h = 15*(12 - \mathrm{LST})$, $\mathrm{LST} = \mathrm{GMT} - \mathrm{longitude}/15$, GMT is the Greenwich time, φ is the latitude, and δ is the solar slant angle. The variables d and δ are calculated with the following equations:

$$\delta = -23.4*\cos(360*(D + 10)/365) \tag{5}$$

$$\begin{aligned} d = {} & 1.00011 + 0.034221\cos(2\pi D/365) \\ & + 0.00128\sin(2\pi D/365) + 0.000719\cos(4\pi D/365) \\ & + 7.7*10^{-5}*\sin(4\pi D/365) \end{aligned} \tag{6}$$

where D is the Julian day for 1 year.

Only part of the solar radiation that is incident on the top of the atmosphere ultimately reaches the Earth's surface due to absorption and reflection by atmospheric components. Rayleigh scattering, absorption by water vapor and other gases, and the effect of aerosol extinction reduce the amount of solar radiation that reaches the Earth's surface. The land surface then reflects some of this radiation back into the atmosphere. That part of this reflected radiation that is not absorbed or scattered by atmospheric gases and aerosols is captured by satellite sensors. The relationship of the radiation observed by satellite sensors, the atmospheric conditions and the land surface reflectance can be described by the atmospheric radiative transfer model. For a uniform, Lambertian surface, the model can be expressed by the classic formula (Liang, 2004):

$$\begin{aligned} L_\lambda(\theta_s, \theta_v, \varphi, \mathrm{atm}) = {} & L_\lambda^0(\theta_s, \theta_v, \varphi, \mathrm{atm}) \\ & + \frac{\rho_\lambda \cdot L_\lambda^{\mathrm{TOA}} \cdot T_{\lambda,\mathrm{d}}(\theta_s, \mathrm{atm}) \cdot T_{\lambda,\mathrm{u}}(\theta_v, \mathrm{atm})}{\pi(1 - s_\lambda(\mathrm{atm}) \cdot \rho_\lambda)} \end{aligned} \tag{7}$$

where $L_\lambda(\theta_s, \theta_v, \varphi, \mathrm{atm})$ is the observed TOA radiance with wavelength λ at the viewing zenith angle θ_v, solar zenith angle θ_s, relative azimuth angle φ and atmospheric condition atm; L_λ^{TOA} is the TOA radiance from the Sun; $L_\lambda^0(\theta_s, \theta_v, \varphi, \mathrm{atm})$ is path radiance without the surface contributions, $T_{\lambda,\mathrm{d}}(\theta_s, \mathrm{atm})$ is the total transmittance from the top of the atmosphere to the

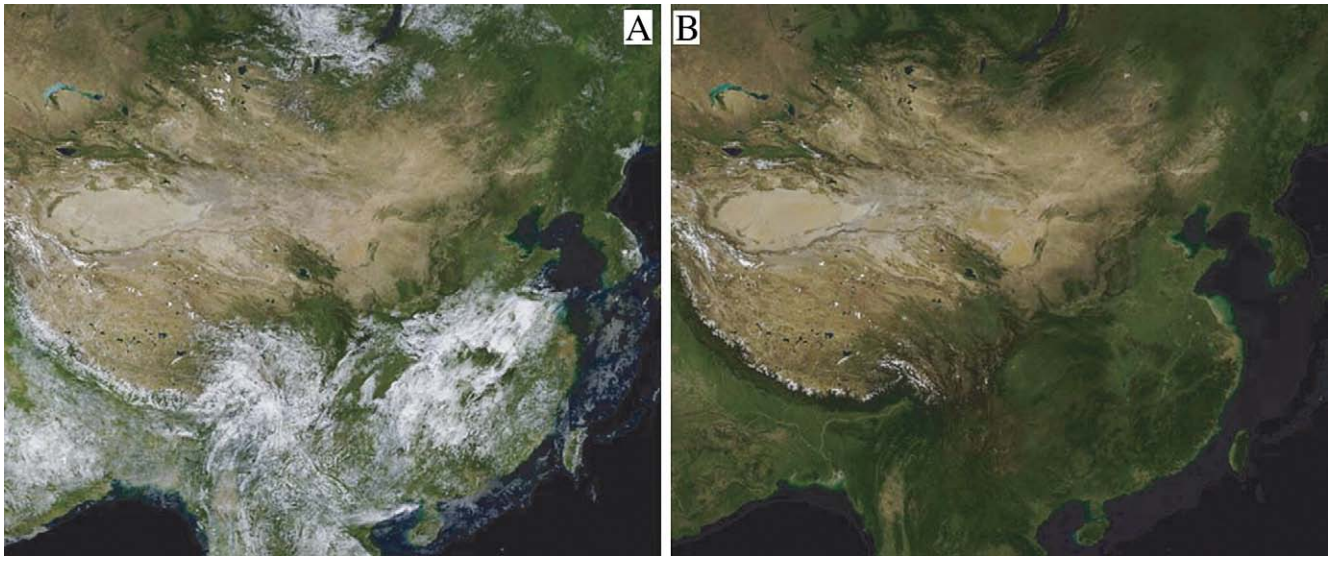

Fig. 1. Multi-temporal interpolation to replace cloud and noise pixels. A is an 8-day, band 1, 4, 3 composite image of Julian day 225, 2003. B is the image after noise removal.

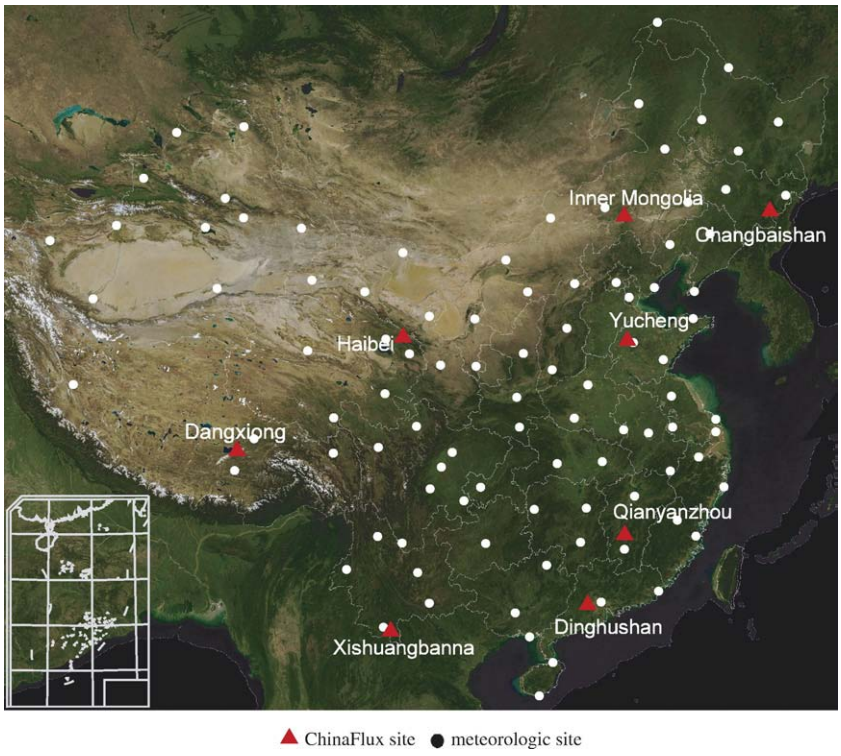

Fig. 2. Location of ChinaFLUX and meteorological station validation sites in China.

surface, $T_{\lambda,u}(\theta_v, \text{atm})$ is the total transmittance from the surface to the sensor, $s_\lambda(\text{atm})$ is the spherical albedo of the atmosphere, and ρ_λ is the land surface reflectance for wavelength λ. Eq. (7) is not valid technically for bi-directional properties of the surface reflectance, but their values can be approximated for the relevant solar and satellite viewing geometries.

If ρ_λ is known, the atmospheric parameters can be calculated from satellite radiance $L_\lambda(\theta_s, \theta_v, \varphi, \text{atm})$ and Eq. (7). A combination of these atmospheric parameters and the land albedo for PAR, direct PAR, diffuse PAR and total PAR can be determined with the atmospheric radiative transfer model. NASA MODIS atmospheric products MOD04/MYD04 (aerosol), MOD05/MYD05 (vapor), MOD06/MYD06 (cloud) and MOD07/MYD07 (ozone) can be used directly as input for PAR estimation (Van Laake & Sanchez-Azofeifa, 2004). However, the uncertainties of the products affect the final PAR results, typically enlarging the error. To minimize the uncertainties from intermediate atmospheric parameters retrieval, two steps are integrated to estimated PAR from TOA radiance and land surface reflectance directly. First, the atmospheric condition is

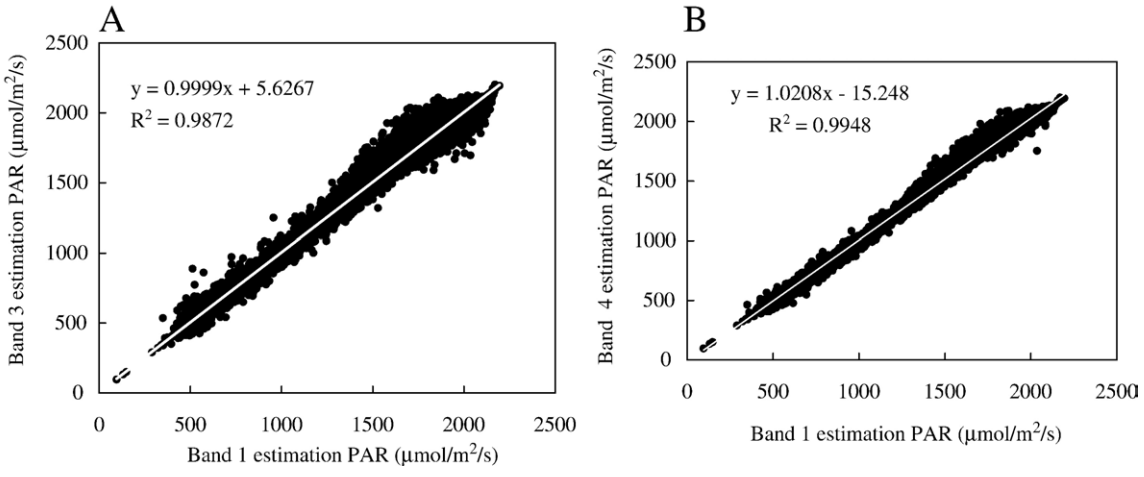

Fig. 3. Comparison of PAR retrievals from single band. (A) Is the comparison of PAR retrieved from bands 3 and 1, (B) is the comparison of PAR retrieved from bands 4 and 1. The dashed line is the regression line and the regression equation is also given in each plot.

Table 1
ChinaFLUX stations

Site	Location	Land cover
Changbaishan	(128.0958, 42.4025)	Needle & broadleaf mixture
Qianyanzhou	(115.0667, 26.7333)	Man-made forest
Dinghushan	(112.5333, 23.1667)	Evergreen broadleaf
Xishuangbanna	(101.2000, 21.9500)	Tropical forest
Haibei	(101.3000, 37.6000)	Steppe
Inner Mongolia	(117.4500, 43.5000)	Grass
Yucheng	(116.6000, 36.9500)	Crops
Dangxiong	(91.0833, 30.8500)	Grass

retrieved by inversion of Eq. (7) with a combination of the land surface ρ_λ and TOA radiance $L_\lambda(\theta_s, \theta_v, \varphi, \text{atm})$ as input. ρ_λ is calculated by compositing several days of mostly clear-sky pixels on the assumption that sky conditions are constant over short-time periods, with the exception of some rapid events such as rain, snow, and fires. Second, diffuse PAR, direct PAR and total PAR are estimated using the atmospheric condition and land surface albedo as input.

3.2. Searching LUT for calculating incident PAR

The atmospheric radiative transfer model simulating Eq. (7) is so slow that it cannot be run operationally at the pixel level. Usually, the pre-calculation parameters are tabled offline as look-up tables. Two look-up tables are created. One describes the relationship of the satellite observational radiance with view zenith angle, relative azimuth angle, solar zenith angle and atmospheric conditions, that is used to estimate atmospheric conditions. The atmospheric conditions include visibility, aerosol type for cloudless skies or cloud type for cloudy sky. The other look-up table describes the function of diffuse PAR, direct PAR with atmospheric conditions, solar zenith, and land surface albedo. To simplify the look-up table procedure, the ozone and vapor absorption are calculated before look-up-table construction. MODTRAN (Berk et al., 1998) is used as the atmospheric radiative transfer model in this paper.

If we know the surface reflectance ρ_i (i=1, 2,...7) for each pixel, for every variation in visibility of the atmosphere in the look-up table, the TOA radiance $\hat{L}_i$ for these N bands can be predicted from a corresponding look-up table. The satellite observing TOA radiance L_i is then compared with $\hat{L}_i$ to determine visibility using linear interpolation to calculate atmospheric conditions. These conditions, combined with land albedo, are then used as input to search the PAR look-up table to retrieve PAR. One atmospheric condition is determined for each band. Because of the possible uncertainties from the input data and various assumptions, the resulting atmospheric conditions from different visible bands are typically different. Two schemes are used to estimate the PAR value (Liang et al., 2006).

3.2.1. Scheme 1

Find the best fitting atmospheric conditions from the results for the seven bands. Because aerosol models and cloud type selections are crucial for retrieval of visibility, the best-fit method was used to find the best visibility and atmospheric type that produces the minimum value of f(atm):

$$f(\text{atm}) = \sum_{i=1}^{N} (L_i - \hat{L}_i)^2 / w_i \tag{8}$$

where w_i is a weight that is assigned to each respective observation. The value of w_i is either 1 or L_i. Atmospheric conditions (cloud and aerosol model types) and visibility are estimated with Eq. (9). PAR is estimated from the PAR look-up table by combining the optimized atmospheric condition with the land surface albedo.

3.2.2. Scheme 2

Usually the best-fit method to determine the atmospheric conditions is complex and slow. A simpler method is to determine the visibility and atmospheric conditions for each band and then to compute PAR by calculating the average after summing over all bands. Thus, the final PAR is the average value for these bands.

$$\text{PAR} = \frac{1}{N} \sum_{i=1}^{N} \text{PAR}^{(i)} \tag{9}$$

We compared the retrieved PAR from the different single band at the 98 meteorological stations sites in China from April 4 to August 25, 2003 (Fig. 2). The estimated PAR values are consistent between the single shortwave bands (Fig. 3). Our analysis indicates that this method achieves good results with only one band. It also demonstrates that Schemes 1 and 2 should yield similar results in most cases. We use Scheme 2 to produce the PAR product.

3.3. Daily integrated PAR estimation

The PAR retrieved from MODIS data is only the instantaneous value. The daily integrated PAR is needed by the ecosystem models to estimate Gross Primary Productivity (GPP). If the atmospheric condition is unchanged over the course of one day, daily PAR is calculated by integration of instantaneous PAR from sunrise to sunset. Although atmospheric conditions sometimes change, generally atmospheric conditions are similar during the morning and afternoon. Whenever MODIS data are available for both morning and afternoon satellite passovers, MODIS/Terra data is used to determine morning atmospheric conditions and MODIS/Aqua data is used to estimate afternoon conditions. In order to represent the change of atmospheric conditions as accurately as possible, each pixel is identified as cloudy or cloudless. If the morning and afternoon pixels reflect differing atmospheric conditions, the daily PAR is the summation of the integrated PAR of the two periods. Otherwise, the atmospheric visibility for a half-hour interval is interpolated from two observational values. These interpolated visibilities are used to estimate diffuse PAR and direct PAR. Then these PARs are summed to calculate the daily PAR. Some high latitude locations are observed by Terra and Aqua multiple times a day. The accuracy

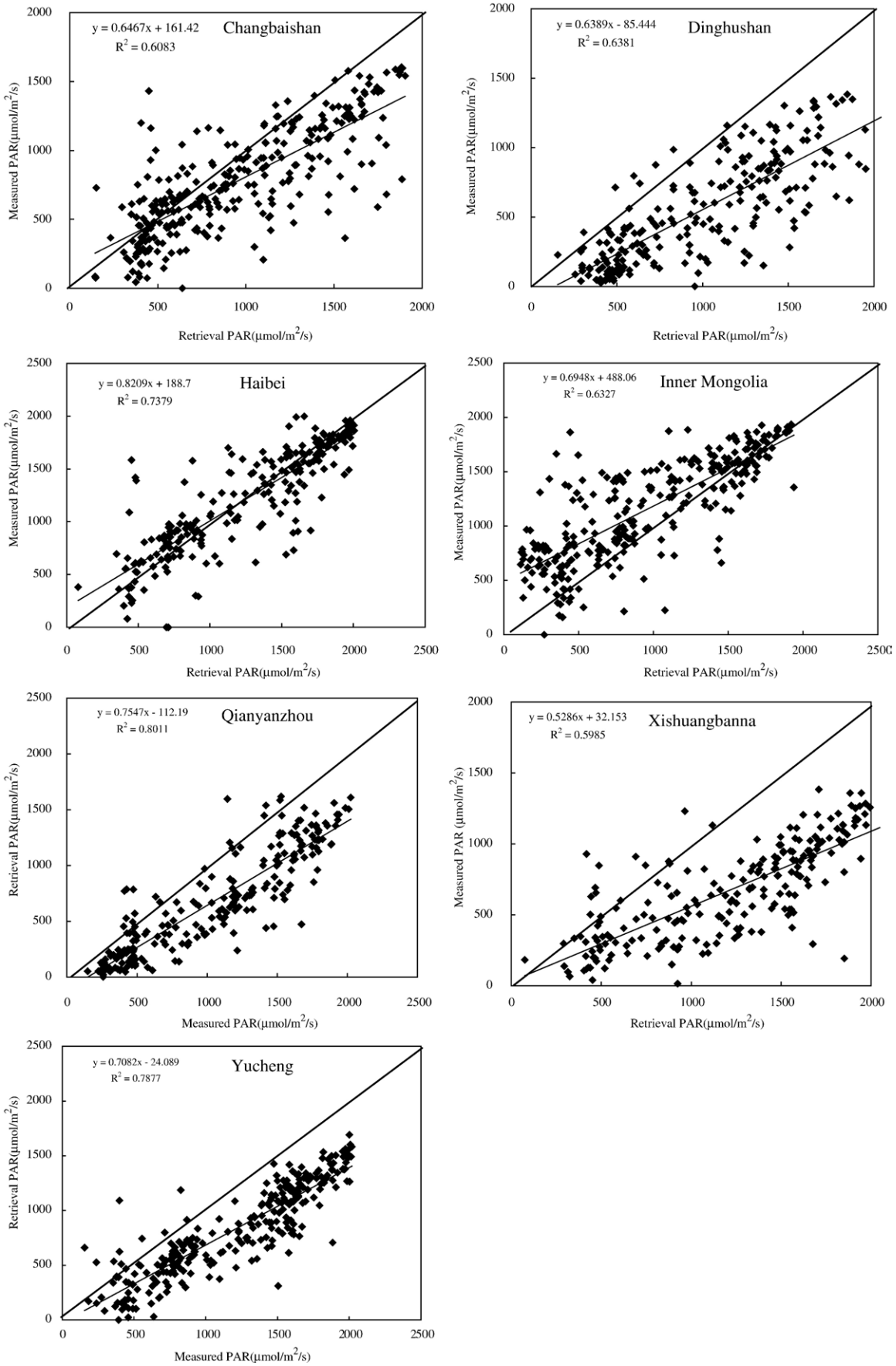

Fig. 4. Validating instantaneous PAR using ChinaFLUX measurements. The thick line is the 1:1 line. The thin line is the regression line and the regression equation is also given in each plot.

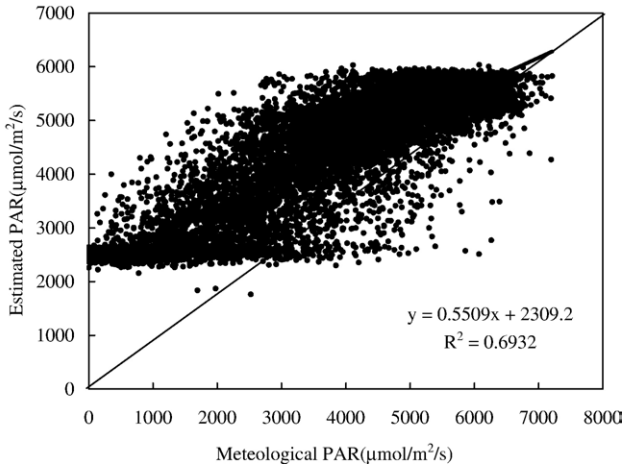

Fig. 5. Comparison of retrieved daily integrated PAR with PAR estimated from meteorological measurements. The thin line is the 1:1 line. The thick line is the regression line and the regression equation is given.

of the daily estimate of PAR for high latitude locations increases because atmospheric conditions are more accurately calculated as the number of satellite passovers increases. If only one satellite observation is available, the snapshot atmospheric conditions are used for a whole day to integrate daily PAR.

4. Results and validation

We use two kinds of measured data to validate estimated PAR values. Instantaneous PAR values are compared with the PAR data measured every half-hour at the seven ChinaFLUX stations. Daily PAR is compared with meteorological measurements.

4.1. Validation instantaneous PAR with ChinaFLUX data

The Chinese Terrestrial Ecosystem Flux Observational Research Network (ChinaFLUX, http://www.chinaflux.org) is a long-term network which relies on Chinese Ecosystem Research Network (CERN). ChinaFLUX uses eddy covariance of micrometeorology and chamber methods as the main research methods to study fluxes of carbon dioxide, water and heat between vegetation and the atmosphere in ecosystems. ChinaFLUX consists of eight sites that use micrometeorological methods and seventeen sites that use the chamber method. The current micrometeorological observational network includes four forest sites (Changbaishan, Qianyanzhou, Dinghushan and Xishuangbanna), three grassland sites (Haibei, Inner Mongolia and Dangxiong) and one cropland site (Yucheng) (Table 1 and Fig. 2).

The Changbaishan site is located on the northern slope of Changbaishan Mountain. Changbaishan Mountain has a temperate continental climate influenced by monsoons with the prominent characteristics of mid-latitudinal upland climate. The area has four distinctly different seasons: a windy spring, a hot and rainy summer, a cool autumn, and a cold winter. Mean annual temperature is 3.6 °C. Mean annual precipitation is 713 mm and most precipitation falls during the summer. The mean annual frost-free period is ~109–141 days and mean annual sunshine duration is ~2271–2503 h.

The Qianyanzhou site is located in the typical red-earth, hilly region in the mid-subtropical monsoon landscape zone of South China. The Qianyanzhou site has a typical sub-tropical monsoon climate. Mean annual air temperature is 18.6 °C. Mean annual precipitation is 1488.8 mm and evaporation is 1110.3 mm. The mean annual sunshine duration is 1785 h, the percentage of sunshine is 44%. Mean annual global radiation is 4349 MJ m^{-2}. The mean annual frost-free period is 323 days.

The Dinghushan site is located in the Dinghushan biosphere reserve of Guangdong province of southern China and is characterized by low mountains and hills. Its climate is most affected by the humid monsoon climate of the torrid zone of south Asia. Mean annual temperature is 21 °C. Mean annual precipitation is 1,956 mm. Rainfall has a distinct pattern of alternating wet and dry seasons. April through September represents the rainy season, November through January represents the dry season. Relative humidity is high and fairly constant throughout the year, and mean annual relative humidity is 82%.

The Xishuangbanna site is a small basin surrounded by low hills and a number of streams located in the National Nature Reserve of the Xishuangbanna Autonomous Prefecture. The climate is tropical monsoon. There are three seasons: foggy and cool, dry and hot, and a rainy season without frost. The mean annual sunshine duration is 1859 h and mean annual air temperature is 21.5 °C. The mean annual precipitation is 1493 mm, mostly occurring during the rainy season from May to October. The mean annual number of foggy days is 186 days.

The Haibei site is located in the northeastern part of the Qinghai–Tibetan Plateau, just east of Qilian Mountain within the Menyuan Hui Autonomous County in the Haibei Zang Autonomous State of Qinghai Province. The altitude is 3200–3600 m. Flood plains and low hills are the dominant landscapes at this site. The climate is characterized by the highland continental climate which is very cold and humid. There are two clearly defined seasons: a very long cold winter and very short warm summer. Mean annual temperature is only −1.7 °C. Annual precipitation is about 600 mm with most precipitation falling in summer. Because it is situated in the frigid highland, the Haibei site receives elevated levels of solar radiation; the mean annual global solar radiation is ~6000–7000 MJ m^{-2}.

The Yucheng site is located in Yucheng County of Shandong Province, eastern China. The dominant landform in this area is the Yellow River alluvial plain with an average elevation of about 28 m. The climate at the Yucheng site is similar to that of the Huang–Huai-Hai Plain. This area is in the warmer temperate zone and the Yucheng site has a semi-humid monsoon climate. Mean annual global solar radiation is 5225 MJ m^{-2}. The mean annual temperature is 13.1 °C and mean annual precipitation is 528 mm. The Yucheng site has abundant sunlight, heat, and ground water.

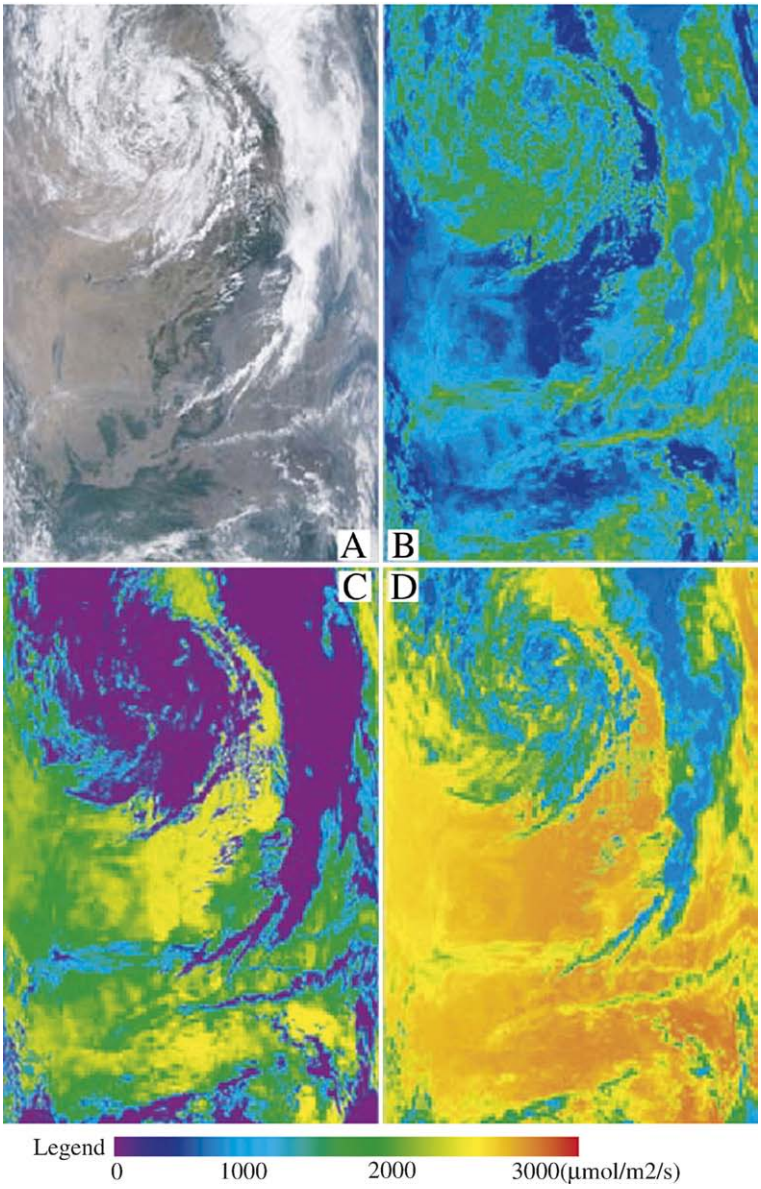

Fig. 6. Instantaneous PAR mapping. A is the band 1, 4, 3 composite MODIS image at UMT 03:24, Julian day 164, 2005. B, C, D are the retrieved diffuse PAR, direct PAR and total PAR from the corresponding MODIS image A respectively.

The Inner Mongolia site is located in the Xilin River Basin, in the southeast part of the Mongolian Plateau. The site ranges in elevation from 950–1500 m. The climate is classified as temperate semi-arid continental. Mean annual temperature is about −0.4 °C. Mean annual precipitation is around 350 mm with large annual fluctuation from 180 – 500 mm. The mean annual frost-free period is about 100 days. For more information about these sites see Yu et al. (2006).

PAR is routinely measured with a quantum sensor (LICOR Inc. LI190SB) at the sites. The validations were conducted using ground measurements of PAR during the entire year of 2005 at eight sites (PAR data is unavailable in here for the Dangxiong site). A 2*2 window of the 1 km MODIS TOA radiance (MOD02) and angular values were extracted from the MODIS 1B data for each site. The ground measurements, collected every half-hour, were compared with the retrieved values. The measurement values closest to the MODIS data acquisition time were used without any interpolation. Fig. 4 shows the comparison of the ground measurements and retrieved values. The comparison shows that the retrieval PARs from grass and crop sites are generally more accurate than those for the forest sites. Forest reflectances may be more difficult to estimate because of a greater BRDF effect. Estimated PAR is less than ground measured PAR for low PAR values that represent thick clouds or aerosols. This may be due to the atmospheric radiative transfer model that underestimates the radiation in these circumstances. Other biases are that the two datasets are mismatched in space and time. For example, the ground observed data is the mean value of data measured every half-hour but the retrieval PAR is an instantaneous value. The

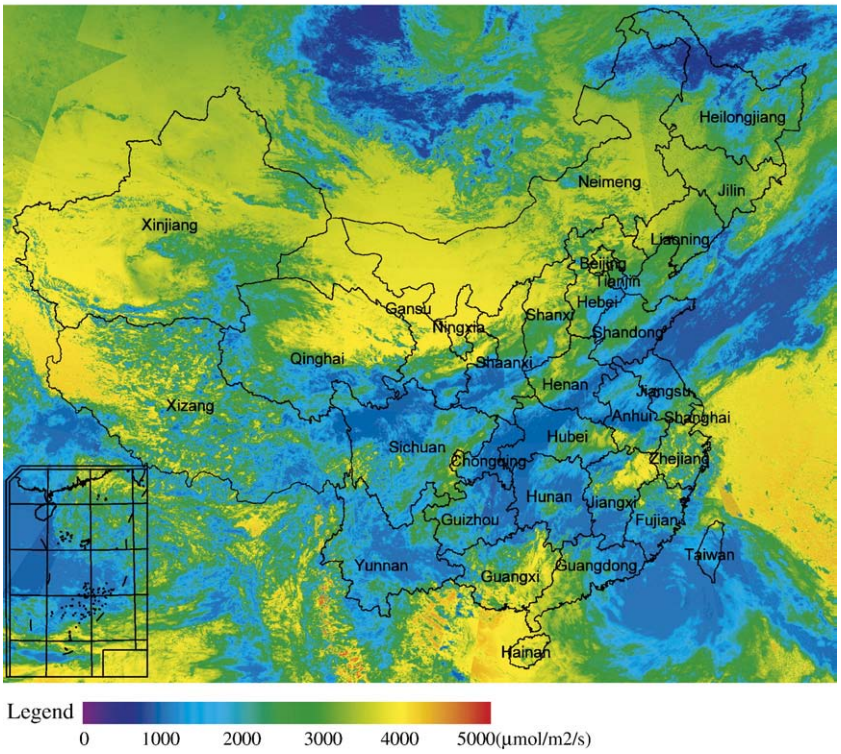

Fig. 7. Daily integrated PAR over China from both Terra and Aqua MODIS data for Julian day 245, 2005.

cloud shadow effect, which underestimates PAR, is also an important contribution to the bias.

4.2. Validation daily integrated PAR with Chinese meteorological radiation data

To investigate the daily PAR over the entire land surface of China, the retrieved daily PAR are also compared with PAR estimated from global radiation measured by 98 meteorological stations distributed across China (Fig. 2). Global radiation is converted to PAR by multiplying by 0.47. The instantaneous PAR at these sites are calculated from 2*2 window pixels with 1 km MODIS data and then integrated to produce daily PAR. This comparison, shown in Fig. 5, indicates that the daily PAR values generally contain large uncertainties when there are only a small number of observations. In addition, this approach overestimated PAR for low values of PAR.

4.3. Mapping PAR in Chinese region

The algorithm described above has been used to process MODIS 1B data to produce instantaneous PAR and daily PAR over China. Fig. 6 is an instantaneous PAR map from MODIS 1B granule at GMT 03:20 of Julian day 164, 2005. The true color composite image (using bands 1, 3 and 4) is shown in Fig. 6(A), and the estimated corresponding diffuse PAR, direct PAR and total PAR are shown in Fig. 6(B), (C) and (D) respectively. It is clear there is a very strong correlation between the original image and the mapped PAR based on the matching patterns. Fig. 7 shows an example of an integrated PAR map of Julian day 245, 2003. The map shows that PAR is low in central China during the day because of the cloud effect.

5. Summary and conclusion

PAR is an important parameter for modeling the atmosphere–terrestrial ecosystem interaction. We have presented an operational approach for calculating retrieved PAR over China from MODIS imagery. This method is based on the idea proposed by Liang et al. (2006) in which PAR is estimated directly from satellite observed radiance in combination with land surface reflectances that can minimize the uncertainties derived from interim production. A new aspect of this method is that the land surface reflectances are estimated from MODIS MOD09/MYD09 and MOD43 products. This avoids the contamination of aerosols or long-term cloud cover on land surface reflectance. This method can separate direct and diffuse components of incident PAR by its use of look-up tables from the MODTRAN radiative transfer package.

Instantaneous PAR has been validated using observations from seven ChinaFLUX stations. The validation results indicate that the results are better for grass sites than forest sites. Comparison of daily PARs with those estimated from the global radiation of 98 meteorological stations shows that this method overestimates PAR for low par values. The system can process MODIS 1B data to generate PAR.

Our analysis demonstrates that it is possible to retrieve PAR from a single band by this method. We base this conclusion on the fact that the retrieved PAR values for each of the seven bands are very similar. For example, GOES stationary data has only one visible band, making it difficult to determine the aerosol type from satellite data only (Wang et al., 2003). This is certain to introduce a large bias in atmospheric conditions retrieval. But this uncertainty in intermediate products can be eliminated by the new method.

MODIS estimates of incident PAR are instantaneous; the daily total PAR is based on the assumption of atmospheric conditions remaining unchanged for half day periods. However, atmospheric conditions usually change rapidly, especially on cloudy days. The Terra and Aqua MODIS sensors may not provide enough information for accurate daily estimation of PAR. A combination of MODIS and geostationary data, such as GOES, FY-2, GMS, is potentially useful to capture the daily cycle of PAR. Geostationary data can provide the daily circle curve and the MODIS data characterizes more details about land surface albedo and aerosol properties. We plan to produce and distribute the Chinese daily PAR from the combination of MODIS and FY-2/GMS in the Resources and Environment Scientific Data Center, Chinese Academy of Sciences.

Acknowledgment

This research is supported in part by the National Natural Science Foundation of China (No. 40471098) and National 973 program (No. 2002CB4125), and NASA under grants NNG05G D10G and NAG512892. The authors would like to thank the ChinaFLUX program, the investigators of the seven stations where the *in situ* measurements were provided for validation, the anonymous reviewers for their valuable comments that have greatly improved this paper, and Dr. Alex Riter for smoothing the English. Any use of the data and images is for descriptive purposes only and does not imply endorsement by the Chinese Government.

References

Berk, A., Bernstein, L. S., Anderson, G. P., Acharya, P. K., Robertson, D. C., Chetwynd, J. H., et al. (1998). MODTRAN cloud and multiple scattering upgrades with application to AVIRIS. *Remote Sensing of Environment*, *65*, 367−375.

Borde, R., & Verdebout, J. (2003). Remote sensing of aerosols optical thickness over various sites using SeaWiFS or VEGETATION and ground measurements. *Remote Sensing of Environment*, *86*(1), 42−51.

Chameides, W. L., Yu, H., Liu, S. C., Bergin, M., Zhou, X., Mearns, L., et al. (1999). Case study of the effects of atmospheric aerosols and regional haze on agriculture: An opportunity to enhance crop yields in China through emission controls. *Proceedings of the National Academy of Sciences*, *vol. 96*. (pp. 13626−13633).

Cohan, D. S., Xu, J., Greenwald, R., Bergin, M. H., & Chameides, W. L. (2002). Impact of atmospheric aerosol light scattering and absorption on terrestrial net primary productivity. *Global Biogeochemical Cycles*, *16*(4), 1090. doi:10.1029/2001GB001441

Dye, D. G., & Shibasaki, R. (1995). Intercomparison of global PAR data sets. *Geophysical Research Letters*, *22*(15), 2013−2016.

Fang, J., Chen, A., Peng, C., Zhao, S., & Ci, L. (2001). Changes in forest biomass carbon storage in China between 1949 and 1998. *Science*, *292*, 2320−2322.

Frouin, R., & Pinker, R. (1995). Estimating photosynthetically active radiation (PAR) at the earth's surface from satellite observations. *Remote Sensing of Environment*, *51*(1), 98−107.

Graham, E. A., Mulkey, S. S., Kitajima, K., Phillips, N. G., & Wright, S. J. (2003). Cloud cover limits net CO_2 uptake and growth of a rainforest tree during tropical rainy seasons. *Proceedings of the National Academy of Sciences*, *100*(2), 572−576.

Gu, J., & Smith, E. A. (1997). High-resolution estimates of total solar and PAR surface fluxes over large-scale BOREAS study area from GOES measurements. *Journal of Geophysical Research*, *102*(D24), 29685−29706.

Gu, L., Baldocchi, D. D., Wofsy, S. C., Munger, J. W., Michalsky, J. J., Urbanski, S. P., et al. (2003). Response of a deciduous forest to the Mount Pinatubo eruption: Enhanced photosynthesis. *Science*, *299*, 2035−2038.

Hauser, A., Oesch, D., Foppa, N., & Wunderle, S. (2005). NOAA AVHRR derived aerosol optical depth over land. *Journal of Geophysical Research*, *110*, D08204. doi:10.1029/ 2004JD005439

Hsu, N. C., Tsay, S. I., King, M. D., & Herman, J. R. (2004). Aerosol properties over bright-reflecting source regions. *IEEE Transactions on Geoscience and Remote Sensing*, *42*(3), 557−569.

Liang, S. (2004). *Quantitative remote sensing of land surfaces.* New York: John Wiley & Sons Inc 534 pp..

Liang, S., Zheng, T., Liu, R., Fang, H., Tsay, S. -C., & Running, S. (2006). Estimation of incident photosynthetically active radiation from Moderate Resolution Imaging Spectrometer data. *Journal of Geophysical Research*, *111*, D15208. doi:10.1029/2005JD006730

Liu, R., Liu, J. Y., Liang, S., Chen, J. M., & Zhuang, D. (2007). Mapping China using MODIS data: Methods, software and products. *Journal of Remote Sensing*, *11*(5), 719−727.

Lu, X., Liu, R., Liu, J., & Liang, S. (2007). Removal of noise by wavelet method to generate high quality temporal data of terrestrial MODIS products. *Photogrammetric Engineering and Remote Sensing*, *73*(10), 1129−1139.

Monteith, J. L. (1972). Solar radiation and productivity in tropical ecosystems. *Journal of Application of Ecology*, *9*(4), 747−766.

Prince, S. D., & Goward, S. N. (1995). Global primary production: A remote sensing approach. *Journal of Biogeography*, *22*, 2829−2849.

Remer, L. A., Remer, Y. J., Kaufman, D., Tanre, S., Mattoo, D. A., Chu, J. V., et al. (2005). The MODIS aerosol algorithm, products and validation. *Journal of the Atmospheric Sciences*, *62*, 947−973.

Running, S. W., Running, S. W., Nemani, R., Glassy, J. M., & Thornton, P. E. (1999). *MODIS PSN (net photosynthesis) and NPP (net primary productivity) products, MOD17 PSN/NPP Algorithm Technical Basis Document, V3.0.* .

Schaaf, C. B., Gao, F., Strahler, A. H., Lucht, W., Li, X., Tsang, T., et al. (2002). First operational BRDF, albedo nadir reflectance products from MODIS. *Remote Sensing of Environment*, *83*, 135−148.

Sellers, P. J., Los, S. O., Tucker, C. J., Justice, C. O., Dazlich, D. A., Collatz, G. J., et al. (1996). A revised land surface parameterization (SiB2) for Atmospheric GCMs. Part II: The generation of global fields of terrestrial biophysical parameters from satellite data. *Journal of Climate*, *9*, 706−737.

Stanhill, G., & Cohen, S. (2001). Global dimming: A review of the evidence for a widespread and significant reduction in global radiation with discussion of its probable causes and possible agricultural consequences. *Agricultural and Forest Meteorology*, *107*, 255−278.

Streets, D. G., Jiang, K., Hu, X., Sinton, J. E., Zhang, X. -Q., Xu, D., et al. (2001). Recent reductions in China's greenhouse gas emissions. *Science*, *294*, 1835−1836.

Van Laake, P. E., & Sanchez-Azofeifa, G. A. (2004). Simplified atmospheric radiative transfer modeling for estimating incident PAR using MODIS atmosphere products. *Remote Sensing of Environment*, *91*, 98−113..

Vermote, E. F., Saleous, N. Z., & Justice, C. O. (2002). Atmospheric correction of MODIS data in the visible to middle infrared: First results. *Remote Sensing of Environment*, *83*(1-2), 97−111.

Wang, J., Christopher, S. A., Brechtel, F., Kim, J., Schmid, B., Redemann, J., et al. (2003). Geostationary satellite retrievals of aerosol optical thickness during ACE-Asia. *Journal of Geophysical Research*, *108*(23). doi:10.1029/2003JD003580

Winslow, J. C., Hunt, E. R. J., & Piper, S. C. (2001). A globally applicable model of daily solar irradiance estimated from air temperature and precipitation data. *Ecological Modelling*, *143*, 227−243.

Wolfe, R. E., Nishihama, M., Fleig, A. J., Kuyper, J. A., Roy, D. P., Storey, J. C., et al. (2002). Achieving sub-pixel geolocation accuracy in support of MODIS land science. *Remote Sensing of Environment*, *83*(1-2), 31−49.

Xiao, X., Braswell, B. H., Zhang, Q., Boles, S. H., Frolking, S. E., & Moore, B., III (2003). Sensitivity of vegetation indices to atmospheric aerosols: Continental-scale observations in Northern Asia. *Remote Sensing of Environment*, *84*(3), 385−392.

Yu, G. R., Wen, X. F., Sun, X. M., Tanner, B. D., Lee, X., & Chen, J. Y. (2006). Overview of ChinaFLUX and evaluation of its eddy covariance measurement. *Agricultural and Forest Meteorology*, *137*, 125−137.

Zhao, M., Heinsch, F. A., Nemani, R. R., & Running, S. W. (2005). Improvements of the MODIS terrestrial gross and net primary production global data set. *Remote Sensing of Environment*, *95*(2), 164−176.